Available online at www.sciencedirect.com
ScienceDirect
Journal of Organometallic Chemistry 691 (2006) 4850–4862
Journal of Organometallic Chemistry
www.elsevier.com/locate/jorganchem

Synthesis and characterization of bis[dicarboxylatotetraorganodistannoxane] units involving 5-[(*E*)-2-(aryl)-1-diazenyl]-2-hydroxybenzoic acids: An investigation of structures by X-ray diffraction, NMR, electrospray ionisation MS and assessment of in vitro cytotoxicity

Tushar S. Basu Baul [a,*], Wandondor Rynjah [a], Eleonora Rivarola [b], Antonin Lyčka [c], Michal Holčapek [d], Robert Jirásko [d], Dick de Vos [e], Ray J. Butcher [f], Anthony Linden [g,*]

[a] *Department of Chemistry, North-Eastern Hill University, NEHU Permanent Campus, Umshing, Shillong 793 022, India*
[b] *Dipartimento di Chimica Inorganica e Analitica "Stanislao Cannizzaro" Università di Palermo, Viale delle Scienze, Parco D'Orleans II, Edificio 17, 90128 Palermo, Italy*
[c] *Research Institute for Organic Syntheses, Rybitvi 296, CZ-532 18 Pardubice 20, Czech Republic*
[d] *University of Pardubice, Department of Analytical Chemistry, Studentska 95, CZ-532 18 Pardubice, Czech Republic*
[e] *Pharmachemie BV, P.O. Box 552, 2003 RN Haarlem, The Netherlands*
[f] *Department of Chemistry, Howard University, Washington, DC 20059, USA*
[g] *Institute of Organic Chemistry, University of Zurich, Winterthurerstrasse 190, CH-8057 Zurich, Switzerland*

Received 8 June 2006; received in revised form 5 August 2006; accepted 5 August 2006
Available online 12 August 2006

Abstract

Reactions of 5-[(*E*)-2-(aryl)-1-diazenyl]-2-hydroxybenzoic acids (LHH′, where the aryl group is an R-substituted phenyl ring such that for L^1HH': R = H; L^2HH': R = 2′-CH_3; L^3HH': R = 3′-CH_3; L^4HH': R = 4′-CH_3; L^5HH': R = 4′-Cl; L^6HH': R = 4′-Br) with $^nBu_2SnO$ in a 1:1 molar ratio yielded complexes of composition $\{[^nBu_2Sn(LH)]_2O\}_2$. The complexes have been characterized by ^1H, ^{13}C, ^{119}Sn NMR, ESI-MS, IR and ^{119m}Sn Mössbauer spectroscopic techniques in combination with elemental analyses. The crystal structures of $\{[^nBu_2Sn(L^1H)]_2O\}_2$ (**1**), $\{[^nBu_2Sn(L^4H)]_2O\}_2$ (**4**), $\{[^nBu_2Sn(L^5H)]_2O\}_2$ (**5**) and $\{[^nBu_2Sn(L^6H)]_2O\}_2$ (**6**) were determined. The compounds are centrosymmetric tetranuclear bis(dicarboxylatotetrabutyldistannoxane) complexes containing a planar Sn_4O_2 core in which two μ_3-oxo O-atoms connect an Sn_2O_2 ring to two exocyclic Sn-atoms. The four carboxylate ligands display two different modes of coordination where both modes involve bridging of two structurally distinct Sn-atoms. The solution structures were confirmed by ^{119}Sn NMR spectroscopy by observing two tin resonances in compounds **1**, and **4**–**6**. The observed difference between the two tin resonances was about 3 ppm while the differences in ^{13}C resonances were even smaller. Compounds $\{[^nBu_2Sn(L^2H)]_2O\}_2$ (**2**) and $\{[^nBu_2Sn(L^3H)]_2O\}_2$ (**3**) undergo a very complex exchange processes in deuteriochloroform solution. The in vitro cytotoxic activity of compounds **1** and **4** against WIDR, M19 MEL, A498, IGROV, H226, MCF7 and EVSA-T human tumour cell lines is reported.

Keywords: Di-*n*-butyltin; Carboxylates; 5-[(*E*)-2-(Aryl)-1-diazenyl]-2-hydroxybenzoic acid; NMR; ESI-MS; Mössbauer; Crystal structure; Cytotoxic activity

1. Introduction

The design and synthesis of coordination polymers with unusual and tailored structures are fundamental steps in the

* Corresponding authors. Tel.: +91 364 2722626; fax: +91 364 2550486/2721000 (T.S. Basu Baul), Tel.: +41 44 635 4228; fax: +41 44 635 6812 (A. Linden).
E-mail addresses: basubaul@nehu.ac.in, basubaul@hotmail.com (T.S. Basu Baul), alinden@oci.unizh.ch (A. Linden).

0022-328X/$ - see front matter © 2006 Elsevier B.V. All rights reserved.
doi:10.1016/j.jorganchem.2006.08.005

discovery and fabrication of various technologically useful materials [1–4]. The majority of such species have been constructed from organic ligands and metal ions by spontaneous self-assembly and such assemblies have resulted in a host of intriguing structural topologies and has also extensive application in material science [5]. It is well known that bis[dicarboxylatotetraorganodistannoxanes] $\{[R_2Sn(O_2CR')]_2O\}_2$ have been studied extensively because they have useful applications in biology and catalysis [6–9]. In the solid state, four basic structural motifs have been observed for $\{[R_2Sn(O_2CR')]_2O\}_2$ complexes when potential coordination of the carboxylate ligand to tin originates only from the carboxylate oxygen atoms; other motifs arise when other potential donor atoms reside in R′ [10] (Scheme 1). The dominant form is (**I**), but a significant number of structures adopt motifs **II**–**V**. There is a wide representation of both carboxylate and alkyl ligands among the structures, but there is no apparent correlation between the nature of the ligands and the observed structural motif. Most of the compounds with general formula $\{[R_2Sn(O_2CR')]_2O\}_2$ contain a centrosymmetric Sn_2O_2 core which is connected to two exocyclic tin atoms via μ_3-oxo O-atoms to give a

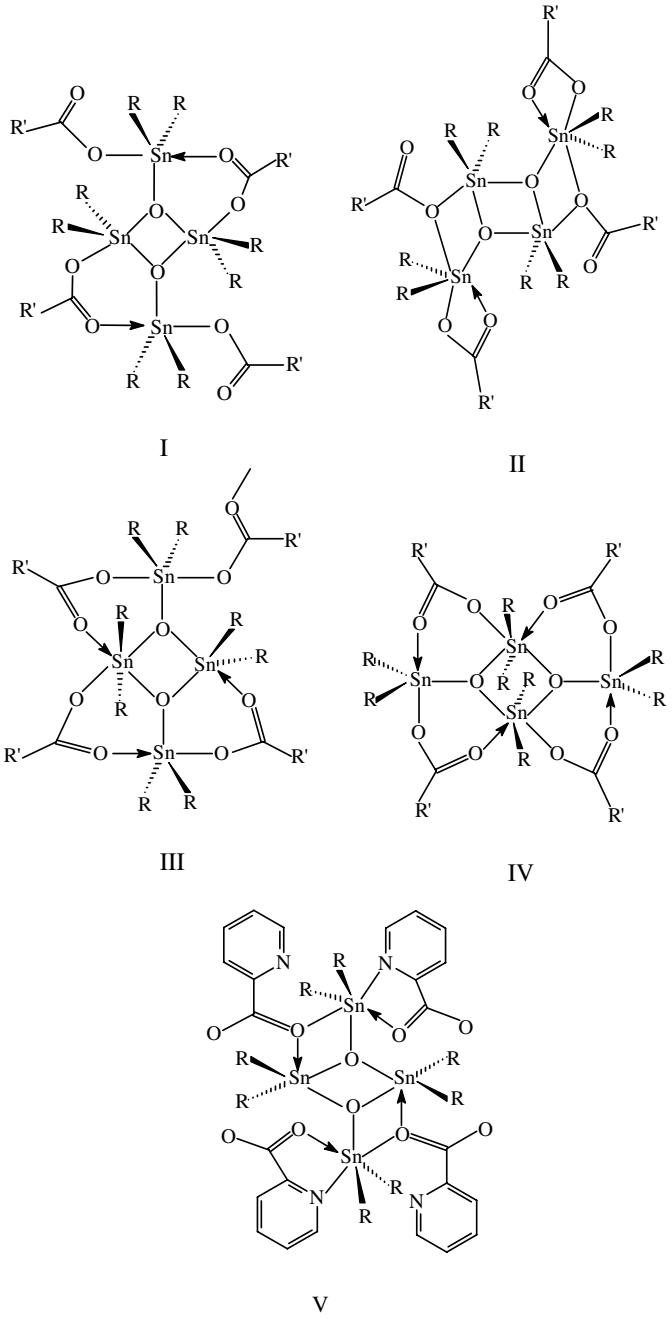

Scheme 1. Various structural motifs in $\{[R_2Sn(O_2CR')_2O]_2\}$ type complexes.

$R_8Sn_4O_2$ central unit. The structural motifs differ from each other in the mode of coordination of the four carboxylate ligands to the $R_8Sn_4O_2$ framework. The coordination geometry around the endo and exocyclic tin atoms varies from distorted trigonal bipyramidal to distorted octahedral, depending on the participating donor atoms (see Scheme 1). In addition to these solid-state studies, ^{119}Sn NMR studies are important for the structure elucidation in solution for an understanding of the chemical properties of $\{[R_2Sn(O_2CR')]_2O\}_2$ complexes, such as their unusual catalytic activity for urethane formation [11]. In this context, several compounds of this class were investigated by ^{119}Sn NMR spectroscopy in order to confirm the geometries around endo- and exocyclic tin atoms, Sn–Sn coupling and thereby the dimeric formulation [12]. The complex structural nature of these $\{[R_2Sn(O_2CR')]_2O\}_2$ compounds provides a useful platform for the investigation of the scope and limitations of ^{119}Sn resonance assignment strategies for structural characterization by 2D gradient-assisted ^{1}H–^{119}Sn HMQC NMR in solution and MAS ^{119}Sn NMR in the solid state [7,13].

Recently, the complexation chemistry of 5-[(*E*)-2-(aryl)-1-diazenyl]-2-hydroxybenzoic acids (Fig. 1) was investigated with (i) triorganotin(IV) complexes of the type R_3SnLH (R = Me, ^{n}Bu, Ph) [14–16] and the reactivities of the products were studied using α-diimine to ascertain the coordination ability to the Sn-complex [16,17] and (ii) diorganotin(IV) complexes of the types $^nBu_2Sn(LH)_2$ [18–20] and $^nBu_2Sn(L^aH \cdot L^bH)_2$ (mixed ligands) [21]. Furthermore, organotin(IV) complexes of this family of carboxylate ligands were investigated for toxicity effects on *Aedes aegypti* mosquito larvae [19] and sea urchin development [17] and in vitro cytotoxicity in human cancer cell lines [20]. In view of the importance of organotin(IV) complexes of this class of ligands and the possible applications of $\{[R_2Sn(O_2CR')]_2O\}_2$ compounds in biology and catalysis, we report further results concerning structural motifs in bis[dicarboxylatotetrabutyldistannoxanes] and their cytotoxic activity in human tumour cell linesin vitro. The complexes have been characterized in the solid state by means of ^{119m}Sn Mössbauer and IR spectroscopic techniques and in solution by ^{1}H, ^{13}C, ^{119}Sn NMR and ESI mass spectrometric studies. The crystal and molecular structures of $\{[^nBu_2Sn(L^1H)]_2O\}_2$ (**1**), $\{[^nBu_2Sn(L^4H)]_2O\}_2$ (**4**), $\{[^nBu_2Sn\text{-}(L^5H)]_2O\}_2$ (**5**), $\{[^nBu_2Sn(L^6H)]_2O\}_2$ (**6**) were also determined in order to elucidate the Sn-coordination modes and environments.

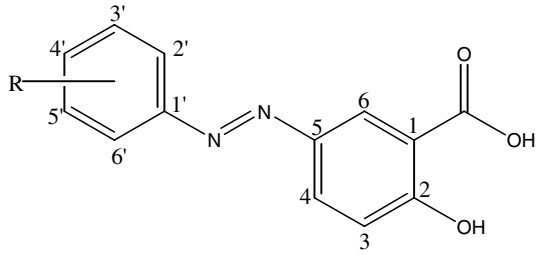

Fig. 1. Ligands used in the present work. Abbreviations: L^1HH': R = H; L^2HH': R = 2′-CH_3; L^3HH': R = 3′-CH_3; L^4HH': R = 4′-CH_3; L^5HH': R = 4′-Cl; L^6HH': R = 4′-Br, where H and H′ represent hydroxy and carboxylic acid protons, respectively.

2. Experimental

2.1. Materials

Di-*n*-butyltin oxide (Fluka) was used as received. The solvents used in the reactions were of AR grade and dried using standard literature procedures.

2.2. Physical measurements

Carbon, hydrogen and nitrogen analyses were performed with a Perkin Elmer 2400 series II instrument. IR spectra in the range 4000–400 cm^{-1} were obtained on a BOMEM DA-8 FT-IR spectrophotometer as KBr discs. The ^{1}H, ^{13}C and ^{119}Sn NMR spectra were recorded on a Bruker ACF 300 spectrometer and measured at 300.13, 75.47 and 111.92 MHz, respectively, or on a Bruker AVANCE 500 spectrometer at 500.13, 125.57 and 186.53 MHz, respectively. The ^{1}H, ^{13}C and ^{119}Sn chemical shifts were referenced to Me_4Si set at 0.00 ppm, $CDCl_3$ set at 77.0 ppm and Me_4Sn set at 0.00 ppm, respectively. Positive-ion and negative-ion electrospray ionization (ESI) mass spectra were measured on an ion trap analyzer Esquire 3000 (Bruker Daltonics, Bremen, Germany) in the range *m*/*z* 50–2500. The samples were dissolved in acetonitrile and analyzed by direct infusion using a flow rate of 5 μl/min. The selected precursor ions were further analyzed by MS/MS analyses under the following conditions: an isolation width of $m/z = 8$ for ions containing one tin atom and $m/z = 12$ for ions containing multiple tin atoms, a collision amplitude in the range 0.7–1.0 V depending on the precursor ion stability, an ion source temperature of 300 °C, and a flow rate and pressure of nitrogen of 4 l/min and 10 psi, respectively. The tuning parameter "compound stability" was set to 100% in the positive-ion mode and 20% in the negative-ion mode. The software IsoPro 3.0 (shareware, http://members.aol.com/msmssoft/) was used for the theoretical calculation of relative isotopic abundances. Mössbauer spectra were recorded on solid samples at liquid nitrogen temperature by using a conventional constant acceleration spectrometer, coupled with a multichannel analyser (a.e.n., Ponteranica (BG), Italy) equipped with a cryostat Cryo (RIAL, Parma, Italy). A $Ca^{119}SnO_3$ Mössbauer source, 10 mCi (from Ritverc, St. Petersburg, Russia) moving at room temperature with constant acceleration in a triangular waveform was used. The velocity calibration was made using a ^{57}Co Mössbauer source, 10 mCi, and an iron foil as absorber (from Ritverc, St. Petesrburg, Russia).

2.3. Synthesis of 5-[(E)-2-(aryl)-1-diazenyl]-2-hydroxybenzoic acids

The 5-[(*E*)-2-(aryl)-1-diazenyl]-2-hydroxybenzoic acids (L^1HH'–L^6HH') were prepared as described in earlier reports [14,15,18,19].

2.4. Synthesis of $\{[^nBu_2Sn(LH)]_2O\}_2$

The dibutyltin(IV) complexes of composition $\{[^nBu_2Sn(LH)]_2O\}_2$ (**1**–**6**) were prepared by the reaction of the appropriate LHH′ with $^nBu_2SnO$ (1:1) in anhydrous toluene under reflux conditions. A typical procedure is described below.

2.4.1. Synthesis of $\{[^nBu_2Sn(L^1H)]_2O\}_2$ (*1*)

A suspension of $^nBu_2SnO$ (0.5 g, 2.064 mmol) and L^1HH' (0.5 g, 2.06 mmol) in 50 ml anhydrous toluene were refluxed for 12 h in a flask equipped with a Dean–Stark water separator and a water cooled condenser. After the reaction, an orange colored solution was obtained and was filtered while hot. The solvent was evaporated *in vacuo*, the orange residue was washed thoroughly with petroleum ether (60–80 °C) and dried *in vacuo*. The residue was dissolved in anhydrous benzene–hexane (v/v 2:1), filtered off to remove any undissolved particles and the filtrate left to crystallize at room temperature. The orange prismatic crystals were isolated from the mother liquor and dried *in vacuo*. Yield: 0.49 g (50%). M.p. 123–125 °C. Anal. Calc. for $C_{84}H_{108}N_8O_{14}Sn_4$: C, 52.31; H, 5.64; N, 5.81. Found: C, 52.24; H, 5.66; N, 5.90%. IR (cm^{-1}): 1625 $\nu(OCO)_{asym}$, 626 ν(Sn–O–Sn). ^1H NMR ($CDCl_3$); δ_H: Ligand skeleton: 7.12 [brs, 1H, H-3], 7.44 [brs, 3H, H-3′, H-4′ and H-5′], 7.89 [brs, 2H, H-2′ and H-6′], 8.12 [brs, 1H, H-4], 8.38 [brs, 1H, H-6], 11.75 [brs, 1H, OH]; Sn–^{n}Bu skeleton: 0.84 [brm, 6H, H-4*], 1.40 [brm, 4H, H-3*], 1.80 [brm, 8H, H-1* and H-2*] ppm. ^{13}C NMR ($CDCl_3$); δ_C: Ligand skeleton: 118.2 [C-1], 119.3[C-3], 122.6 [C-2′ and C-6′], 124.0 [C-6], 126.4 [C-4], 129.0 [C-3′ and C-5′], 130.5 [C-4′], 145.3 [C-5], 152.7 [C-1′], 164.2 [C-2], 175.5 [CO_2]; Sn–^{n}Bu skeleton: 27.7, 27.4, 27.2, 26.7 and 23.9 [C-1*, C-2* and C-3*], 13.5 [C-4*] ppm. ^{119}Sn NMR ($CDCl_3$); δ_{Sn}: −185.4 and −189.7 ppm. ESI-MS: $M_{mono} = 474 = L^1SnBu_2$–H. Positive-ion MS: *m/z* 1462; *m/z* 993 $[M_{mono}+H+OSnBu_2+(OH)_2SnBu_2]^+$; *m/z* 975 $[M_{mono}+H+2*OSnBu_2]^+$; *m/z* 751 $[(OSnBu_2)_3+H]^+$, 100%; *m/z* 725 $[M_{mono}+H+OSnBu_2]^+$; *m/z* 501 $[(OSnBu_2)_2+H]^+$. MS/MS of *m/z* 993: *m/z* 975 $[M_{mono}+H+2*OSnBu_2]^+$; *m/z* 751 $[(OSnBu_2)_3+H]^+$; *m/z* 501 $[(OSnBu_2)_2+H]^+$. MS/MS of *m/z* 725: *m/z* 707 $[M_{mono}+H+OSnBu_2-H_2O]^+$; *m/z* 501 $[(OSnBu_2)_2+H]^+$; *m/z* 387 $[(OSnBu_2)_2+H-butene-butane]^+$; *m/z* 273 $[(OSnBu_2)_2+H-2*butane-2*butene]^+$. Negative-ion MS: *m/z* 1949 $[M-H+H_2O]^-$; *m/z* 1931 $[M-H]^-$; *m/z* 1905 $[3*M_{mono}+L^1+L^1H]^-$; *m/z* 1663 $[3*M_{mono}+L^1]^-$; *m/z* 1457 $[3*M_{mono}+Cl]^-$; *m/z* 1431 $[2*M_{mono}+L^1+L^1H]^-$; *m/z* 1225 $[2*M_{mono}+Cl+L^1H]^-$; *m/z* 1189 $[2*M_{mono}+L^1]^-$; *m/z* 983 $[2*M_{mono}+Cl]^-$; *m/z* 715 $[M_{mono}+L^1]^-$; *m/z* 509 $[M_{mono}+Cl]^-$; *m/z* 241 $[L^1]^-$, 100%; *m/z* 197 $[L^1-CO_2]^-$. MS/MS of *m/z* 1931: *m/z* 1689 $[M-H-L^1H]^-$; *m/z* 1439 $[M-H-H_2O-M_{mono}]^-$; *m/z* 1215 $[M-H-M_{mono}-L^1H]^-$; *m/z* 715 $[M_{mono}+L^1]^-$. ^{119}Sn Mössbauer spectrum: $\delta = 1.31$, $\Delta = 3.23$, $\Gamma_1 = 0.79$, $\Gamma_2 = 0.87$ mm s^{-1}, $\rho = 2.47$, C–Sn–C angle[1]: 134°.

2.4.2. Synthesis of $\{[^nBu_2Sn(L^2H)]_2O\}_2$ (*2*)

Orange block shaped crystals of compound **2**, M.p. 86-88 °C, were obtained from hexane. Yield: 0.3 g (30.9%). Anal. Calc. for $C_{88}H_{116}N_8O_{14}Sn_4$: C, 53.25; H, 5.89; N, 5.65. Found: C, 53.20; H, 5.80; N, 5.70%. IR (cm^{-1}): 1625 $\nu(OCO)_{asym}$, 629 ν(Sn–O–Sn). For NMR: refer to Section 3.2 for specific comments. ESI-MS: $M_{mono} = 488 = L^2SnBu_2$–H. Positive-ion MS: *m/z* 1495 $[2*M_{mono}+H+OSnBu_2+(OH)_2SnBu_2]^+$; *m/z* 1007 $[M_{mono}+H+OSnBu_2+(OH)_2SnBu_2]^+$; *m/z* 989 $[M_{mono}+H+2*OSnBu_2]^+$; *m/z* 751 $[(OSnBu_2)_3+H]^+$, 100%; *m/z* 739 $[M_{mono}+H+OSnBu_2]^+$; *m/z* 501 $[(OSnBu_2)_2+H]^+$. MS/MS of *m/z* 1007: *m/z* 989 $[M_{mono}+H+2*OSnBu_2]^+$; *m/z* 751 $[(OSnBu_2)_3+H]^+$; *m/z* 501 $[(OSnBu_2)_2+H]^+$. MS/MS of *m/z* 739: *m/z* 721 $[M_{mono}+H+OSnBu_2-H_2O]^+$; *m/z* 607 $[M_{mono}+H+OSnBu_2-H_2O-butene-butane]^+$; *m/z* 501 $[(OSnBu_2)_2+H]^+$; *m/z* 387 $[(OSnBu_2)_2+H-butene-butane]^+$; *m/z* 273 $[(OSnBu_2)_2+H-2*butane-2*butene]^+$. Negativeion MS: *m/z* 2005 $[M-H+H_2O]^-$; *m/z* 1987 $[M-H]^-$; *m/z* 1975 $[3*M_{mono}+L^2+L^2H]^-$; *m/z* 1719 $[3*M_{mono}+L^2]^-$; *m/z* 1487 $[2*M_{mono}+L^2+L^2H]^-$; *m/z* 1267 $[2*M_{mono}+Cl+L^2H]^-$; *m/z* 1231 $[2*M_{mono}+L^2]^-$; *m/z* 1011 $[2*M_{mono}+Cl]^-$; *m/z* 999 $[M_{mono}+L^2+L^2H]^-$; *m/z* 779 $[M_{mono}+L^2+HCl]^-$; *m/z* 743 $[M_{mono}+L^2]^-$; *m/z* 523 $[M_{mono}+Cl]^-$; *m/z* 255 $[L^2]^-$, 100%; *m/z* 211 $[L^2-CO_2]^-$. MS/MS of *m/z* 1987: *m/z* 1969 $[M-H-H_2O]^-$; *m/z* 1731 $[M-H-L^2H]^-$; *m/z* 1481 $[M-H-H_2O-M_{mono}]^-$; *m/z* 1243 $[M-H-M_{mono}-L^2H]^-$; *m/z* 743 $[M_{mono}+L^2]^-$. ^{119}Sn Mössbauer spectrum: $\delta = 1.35$, $\Delta = 3.49$, $\Gamma_1 = 0.82$, $\Gamma_2 = 0.82$ mm s^{-1}, $\rho = 2.59$, C–Sn–C angle[1]: 142°.

2.4.3. Synthesis of $\{[^nBu_2Sn(L^3H)]_2O\}_2$ (*3*)

Orange crystals of compound **3**, Yield: 0.35g (35.4%). M.p. 70–72 °C. Anal. Calc. for $C_{88}H_{116}N_8O_{14}Sn_4$: C, 53.25; H, 5.89; N, 5.65. Found: C, 53.20; H, 5.80; N, 5.75%. IR (cm^{-1}): 1625cm^{-1} $\nu(OCO)_{asym}$, 630 ν(Sn–O–Sn). For NMR: refer to Section 3.2 for specific comments. ESI-MS: $M_{mono} = 488 = L^3SnBu_2$–H. Mass spectra were found to be identical as that for compound **2**. ^{119}Sn Mössbauer: $\delta = 1.31$, $\Delta = 3.23$, $\Gamma_1 = 0.83$, $\Gamma_2 = 0.83$ mm s^{-1}, $\rho = 2.47$, C–Sn–C angle[1]: 134°.

2.4.4. Synthesis of $\{[^nBu_2Sn(L^4H)]_2O\}_2$ (*4*)

Orange prismatic crystals of compound **4**, M.p. 135-137 °C, were obtained from benzene–hexane (v/v 2:1). Yield: 0.5 g (51.6%). Anal. Calc. for $C_{88}H_{116}N_8O_{14}Sn_4$:

[1] C–Sn–C angle (median values) were calculated for six-coordinated structures from Q.S. values.

C, 53.25; H, 5.89; N, 5.65. Found: C, 53.20; H, 5.90; N, 5.70%. IR (cm^{-1}): 1625 $\nu(OCO)_{asym}$, 620 ν(Sn–O–Sn). ^1H NMR ($CDCl_3$); δ_H: Ligand skeleton: 2.43 and 2.37 [br, 6H, CH_3], 7.25 [brs, 3H, H3, H-2′ and H-6′], 7.86 [brs, 2H, H-3′ and H-5′], 8.16 [brs, 1H, H-4], 8.36 [brs, 1H, H-6], 11.7 [brs, 1H, OH]; Sn–^{n}Bu skeleton: 0.85 [brm, 6H, H-4*], 1.40 [brm, 4H, H-3*], 1.80 [brm, 8H, H-1* and H-2*]ppm. ^{13}C NMR ($CDCl_3$); δ_C: Ligand skeleton: 21.4 [CH_3], 114.2 [C-1], 118.2 [C-3], 122.6 [C-2′ and C-6′], 126.3 [C-6], 128.3 [C-4], 129.6 [C-3′ and C-5′], 141.0 [C-4′], 145.4 [C-5], 150.7 [C-1′], 163.9 [C-2], 175.7 [CO_2]; Sn–^{n}Bu skeleton: 27.7, 27.4, 27.2, 26.7 and 23.9 [C-1*, C-2* and C-3*], 13.5 [C-4*] ppm. ^{119}Sn NMR ($CDCl_3$); δ_{Sn}: −186.5 and −187.7 ppm. ESI-MS: $M_{mono} = 488 =$ $LSnBu_2$–H. Mass spectra were found to be identical as that for compound **2**. ^{119}Sn Mössbauer spectrum: $\delta = 1.31$, $\Delta = 3.25$, $\Gamma_1 = 0.84$, $\Gamma_2 = 0.91$ mm s^{-1}, $\rho = 2.48$, C–Sn–C angle[1]: 135°.

2.4.5. Synthesis of $\{[^nBu_2Sn(L^5H)]_2O\}_2$ (5)

Orange prismatic crystals of compound **5**, M.p. 165–166 °C, were obtained from benzene–hexane (v/v 2:1). Yield: 0.7 g (74.4%). Anal. Calc. for $C_{84}H_{104}N_8O_{14}Cl_4Sn_4$: C, 48.82; H, 5.07; N, 5.42. Found: C, 48.90; H, 5.20; N, 5.50%. IR (cm^{-1}): 1625 $\nu(OCO)_{asym}$, 620 ν(Sn–O–Sn). ^1H NMR ($CDCl_3$); δ_H: Ligand skeleton: 7.10 [brs, 1H, H-3], 7.43 [brs, 2H, H-2′ and H-6′], 7.80 [brs, 2H, H-3′ and H-5′], 8.09 [brs, 1H, H-4], 8.37 [brs, 1H, H-6], 11.73 [brs, 1H, OH]; Sn–^{n}Bu skeleton: 0.83 [brm, 6H, H-4*], 1.40 [brm, 4H, H-3*], 1.82 [brm, 8H, H-1* and H-2*]ppm. ^{13}C NMR ($CDCl_3$); δ_C: Ligand skeleton: 114.8 [C-1], 118.4 [C-3], 123.8 [C-2′ and C-6′], 126.6 [C-6], 128.3 [C-4], 129.2 [C-3′ and C-5′], 136.4 [C-4′], 145.2 [C-5], 150.8 [C-1′], 164.4 [C-2], 175.2 [CO_2]; Sn–^{n}Bu skeleton: 27.7, 27.4, 27.2, 26.7 and 26.4 [C-1*, C-2* and C-3*], 13.5 [C-4*] ppm. ^{119}Sn NMR ($CDCl_3$); δ_{Sn}: −186.4 and −188.4 ppm. ESI-MS: $M_{mono} = 508 = L^5SnBu_2$–H. Positive-ion MS: *m/z* 1027 $[M_{mono}+H+OSnBu_2+(OH)_2SnBu_2]^+$; *m/z* 1009 $[M_{mono}+H+2*OSnBu_2]^+$; *m/z* 759 $[M_{mono}+H+OSnBu_2]^+$; *m/z* 751 $[(OSnBu_2)_3+H]^+$, 100%; *m/z* 501 $[(OSnBu_2)_2+H]^+$. MS/MS of *m/z* 1027: *m/z* 1009 $[M_{mono}+H+2*OSnBu_2]^+$; *m/z* 751 $[(OSnBu_2)_3+H]^+$; *m/z* 501 $[(OSnBu_2)_2+H]^+$. MS/MS of *m/z* 759: *m/z* 741 $[M_{mono}+H+OSnBu_2-H_2O]^+$; *m/z* 627 $[M_{mono}+H+OSnBu_2-H_2O-butene-butane]^+$; *m/z* 501 $[(OSnBu_2)_2+H]^+$; *m/z* 387 $[(OSnBu_2)_2+H-butene-butane]^+$; *m/z* 273 $[(OSnBu_2)_2+H-2*butane-2*butene]^+$; *m/z* 251 $[OSnBu_2+H]^+$. MS/MS of *m/z* 751: *m/z* 733 $[(OSnBu_2)_3+H-H_2O]^+$; *m/z* 655 $[(OSnBu_2)_3+H-butene-butane+H_2O]^+$; *m/z* 619 $[(OSnBu_2)_3+H-butene-butane-H_2O]^+$; *m/z* 541 $[(OSnBu_2)_3+H-32*butene-2*butane+H_2O]^+$; *m/z* 523 $[(OSnBu_2)_3+H-32*butene-2*butane]^+$; *m/z* 501 $[(OSnBu_2)_2+H]^+$; *m/z* 465; *m/z* 427 $[(OSnBu_2)_3+H-3*butene-3*butane+H_2O]^+$; *m/z* 409 $[(OSnBu_2)_3+H-3*butene-3*butane]^+$; *m/z* 387 $[(OSnBu_2)_2+H-butene-butane]^+$; *m/z* 273 $[(OSnBu_2)_2+H-2*butane-2*butene]^+$. Negative-ion MS: *m/z* 2085 $[M-H+H_2O]^-$; *m/z* 2075 $[3*M_{mono}+L^5+L^5H]^-$; *m/z* 2067 $[M-H]^-$; *m/z* 1799 $[3*M_{mono}+L^5]^-$; *m/z* 1567 $[2*M_{mono}+L^5+L^5H]^-$; *m/z* 1327 $[2*M_{mono}+Cl+L^5H]^-$; *m/z* 1291 $[2*M_{mono}+L^5]^-$; *m/z* 1059 $[M_{mono}+L^5+L^5H]^-$; *m/z* 1051 $[2*M_{mono}+Cl]^-$; *m/z* 819 $[M_{mono}+L^5+HCl]^-$; *m/z* 783 $[M_{mono}+L^5]^-$, 100%; *m/z* 543 $[M_{mono}+Cl]^-$; *m/z* 275 $[L^5]^-$; *m/z* 231 $[L^5-CO_2]^-$. MS/MS of *m/z* 2067: *m/z* 2049 $[M-H-H_2O]^-$; *m/z* 1791 $[M-H-L^5H]^-$; *m/z* 1541 $[M-H-H_2O-M_{mono}]^-$; *m/z* 1283 $[M-H-M_{mono}-L^5H]^-$; *m/z* 783 $[M_{mono}+L^5]^-$. ^{119}Sn Mössbauer spectrum: $\delta = 1.35$, $\Delta = 3.26$, $\Gamma_1 = 0.83$, $\Gamma_2 = 0.95$ mm s^{-1}, $\rho = 2.41$, C–Sn–C angle[1]: 135°.

2.4.6. Synthesis of $\{[^nBu_2Sn(L^6H)]_2O\}_2$ (6)

Orange prismatic crystals of compound **6**, M.p. 130 °C, were obtained from benzene–hexane (v/v 2:1). Yield: 0.58 g (66.4%). Anal. Calc. for $C_{84}H_{104}N_8O_{14}Br_4Sn_4$: C, 44.96; H, 4.67; N, 4.99. Found: C, 45.07; H, 4.80; N, 5.02%. IR (cm^{-1}): 1625 $\nu(OCO)_{asym}$, 627 ν(Sn–O–Sn). ^1H NMR ($CDCl_3$); δ_H: Ligand skeleton: 7.10 [brs, 1H, H-3], 7.52 [brs, 2H, H-2′ and H-6′], 7.73 [brs, 2H, H-3′ and H-5′], 8.09 [brs, 1H, H-4], 8.36 [brs, 1H, H-6], 11.72 [brs, 1H, OH]; Sn–^{n}Bu skeleton: 0.83 [brm, 6H, H-4*], 1.40 [brm, 4H, H-3*], 1.78 [brm, 8H, H-1* and H-2*] ppm. ^{13}C NMR ($CDCl_3$); δ_C: Ligand skeleton: 112.8 [C-1], 118.4 [C-3], 124.1 [C-2′ and C-6′], 126.6 [C-6], 128.3 [C-4], 129.5 [C-4′], 132.2 [C-3′ and C-5′], 145.1 [C-5], 151.5 [C-1′], 164.4 [C-2], 176.0 [CO_2]; Sn–^{n}Bu skeleton: 27.7, 27.4, 27.2 and 26.7 [C-1*, C-2* and C-3*], 13.5 [C-4*] ppm. ^{119}Sn NMR ($CDCl_3$); δ_{Sn}: −186.8 and −188.2 ppm. ESI-MS: $M_{mono} = 552 = L^6SnBu_2$–H. Positive-ion MS: *m/z* 1071 $[M_{mono}+H+OSnBu_2+(OH)_2SnBu_2]^+$; *m/z* 1053 $[M_{mono}+H+2*OSnBu_2]^+$; *m/z* 803 $[M_{mono}+H+OSnBu_2]^+$; *m/z* 751 $[(OSnBu_2)_3+H]^+$, 100%; *m/z* 501 $[(OSnBu_2)_2+H]^+$. MS/MS of *m/z* 1071: *m/z* 1053 $[M_{mono}+H+2*OSnBu_2]^+$; *m/z* 751 $[(OSnBu_2)_3+H]^+$; *m/z* 501 $[(OSnBu_2)_2+H]^+$. MS/MS of *m/z* 803: *m/z* 785 $[M_{mono}+H+OSnBu_2-H_2O]^+$; *m/z* 671 $[M_{mono}+H+OSnBu_2-H_2O-butene-butane]^+$; *m/z* 501 $[(OSnBu_2)_2+H]^+$; *m/z* 387 $[(OSnBu_2)_2+H-butene-butane]^+$; *m/z* 273 $[(OSnBu_2)_2+H-2*butane-2*butene]^+$; *m/z* 251 $[OSnBu_2+H]^+$. Negative-ion MS: *m/z* 2261 $[M-H+H_2O]^-$; *m/z* 2243 $[M-H]^-$; *m/z* 1975 $[3*M_{mono}+L^6]^-$; *m/z* 1743 $[2*M_{mono}+L^6+L^6H]^-$; *m/z* 1423 $[2*M_{mono}+L^6]^-$; *m/z* 1191 $[M_{mono}+L^6+L^6H]^-$; *m/z* 1139 $[2*M_{mono}+Cl]^-$; *m/z* 871 $[M_{mono}+L^6]^-$, 100%; *m/z* 587 $[M_{mono}+Cl]^-$; *m/z* 319 $[L^6]^-$; *m/z* 275 $[L^6-CO_2]^-$. MS/MS of *m/z* 2243: *m/z* 1923 $[M-H-L^6H]^-$; *m/z* 1673 $[M-H-H_2O-M_{mono}]^-$; *m/z* 1371 $[M-H-M_{mono}-L^6H]^-$; *m/z* 871 $[M_{mono}+L^6]^-$. ^{119}Sn Mössbauer spectrum: $\delta = 1.33$, $\Delta = 3.25$, $\Gamma_1 = 0.88$, $\Gamma_2 = 0.94$ mm s^{-1}, $\rho = 2.44$, C–Sn–C angle[1]: 135 °.

2.5. X-ray crystallography

Crystals of compounds **1** and **4**–**6** suitable for an X-ray crystal-structure determination were obtained from benzene-*n*-hexane (v/v 2:1). All measurements were made at

low temperature and with graphite-monochromated Mo Kα radiation ($\lambda = 0.71073$ Å). For **1** and **5**, a Nonius Kappa CCD diffractometer [22] and an Oxford Cryosystems Cryostream 700 cooler were employed and data reduction was performed with HKL Denzo and Scalepack [23]. Empirical absorption corrections were applied using SORTAV [24], equivalent reflections were merged and the structures were solved by direct methods using SIR92 [25]. For **4** and **6**, a Bruker SMART CCD diffractometer was employed [26] and data reduction was performed with SHELXTL [26]. Empirical absorption corrections were applied using SADABS [26], equivalent reflections were merged and the structures were solved by direct methods using SHELXS97 [27]. For each structure, the non-hydrogen atoms were refined anistropically. In each structure, the molecule of the tetranuclear Sn-complex sits about a crystallographic centre of inversion and the non-hydrogen atoms were refined anistropically. The crystals of **4** and **5** are 1:1 *n*-hexane and benzene solvates, respectively, in which the solvent molecules also sit across centres of inversion. Compound **6** is also a benzene solvate with the benzene molecules on centres of inversion, but the solvent molecule sites are only partially occupied and the global site occupation factor refined to a value of 0.734(9). The data collection and refinement parameters are given in Table 1. As the molecular structures of the four compounds are quite similar, only views of the molecules of **1** and **6** are shown in Figs. 2 and 3 while views of the molecules of **4** and **5** are deposited as Supplementary material.

In **1**, all of the four unique butyl groups are disordered over two conformations. Two sets of overlapping positions were defined for the terminal ethyl segment in one butyl group [C(33) to C(34)], and for all atoms of the remaining butyl groups. Refinement of constrained site occupation factors for the two orientations of these groups yielded values of 0.70(2) and 0.771(4) for the major conformations about Sn(1) and Sn(2), respectively. Similarity restraints were applied to the chemically equivalent bond lengths and angles involving all disordered C-atoms, while neighbouring atoms within and between each conformation of the disordered butyl groups were restrained to have similar atomic displacement parameters.

In **5**, three of the four unique butyl groups are disordered over two conformations. Two sets of overlapping positions were defined for the terminal propyl segment in one butyl group [C(32) to C(34)], the terminal ethyl segment in the second butyl group [C(37) and C(38)] and the terminal methyl group in the third case [C(42)]. Refinement of constrained site occupation factors for the two orientations of these groups yielded values of 0.509(7), 0.852(7) and 0.551(8), respectively, for the major conformations. Similarity restraints were employed as described for **1**.

In **6**, one butyl group on each of the unique Sn-atoms is disordered over two conformations. Two sets of overlapping positions were defined for all atoms of these butyl groups. Refinement of constrained site occupation factors for the two orientations of these groups yielded values of 0.565(9) and 0.734(9) for the major conformations about

Table 1
Crystallographic data and structure refinement parameters for **1** and **4–6**

	1	**4**	**5**	**6**
Empirical formula	$C_{84}H_{108}N_8O_{14}Sn_4$	$C_{88}H_{116}N_8O_{14}Sn_4 \cdot C_6H_{14}$	$C_{84}H_{104}Cl_4N_8O_{14}Sn_4 \cdot C_6H_6$	$C_{84}H_{104}Br_4N_8O_{14}Sn_4 \cdot 0.734C_6H_6$
Formula weight	1928.22	2070.82	2144.11	2301.14
Crystal size (mm)	$0.12 \times 0.25 \times 0.25$	$0.35 \times 0.40 \times 0.60$	$0.07 \times 0.15 \times 0.20$	$0.46 \times 0.40 \times 0.10$
Crystal shape	Prism	Block	Prism	Plate
Temperature (K)	160(1)	93(2)	160(1)	93(2)
Crystal system	Monoclinic	Triclinic	Triclinic	Triclinic
Space group	$P2_1/c$	$P\bar{1}$	$P\bar{1}$	$P\bar{1}$
a (Å)	13.1703(1)	12.642(2)	13.4700(3)	13.473(2)
b (Å)	26.6686(3)	14.219(2)	14.6505(3)	14.646(2)
c (Å)	12.4420(1)	15.606(3)	14.8915(2)	14.953(2)
α (°)	90	113.154(3)	60.644(1)	60.867(2)
β (°)	97.8817(6)	104.647(3)	68.274(1)	68.693(2)
γ (°)	90	100.809(3)	71.203(1)	71.328(2)
V (Å^3)	4328.76(7)	2362.1(7)	2343.19(8)	2363.6(5)
Z	2	1	1	1
D_x (g cm^{-3})	1.479	1.456	1.519	1.617
μ (mm^{-1})	1.204	1.110	1.231	2.802
Transmission factors (min, max)	0.683; 0.872	0.787; 0.894	0.742; 0.922	0.753; 1.0
$2\theta_{max}$ (°)	60	56.6	60	57
Reflections measured	86,626	19,252	65,420	16,414
Independent reflections (R_{int})	12,653 (0.067)	11,195 (0.037)	13,684 (0.064)	10,934 (0.040)
Reflections with $I > 2\sigma(I)$	9875	7538	9847	8804
Number of parameters	640	548	613	579
Number of restraints	386	0	91	22
$R(F)$ ($I > 2\sigma(I)$ reflections)	0.037	0.038	0.042	0.053
$wR(F^2)$ (all data)	0.086	0.095	0.105	0.140
Goodness-of-fit (F^2)	1.046	0.916	1.029	1.102
Max, min $\Delta\rho$ (e/Å^3)	0.96; −1.17	1.14; −1.03	1.36; −1.22	2.48; −1.74

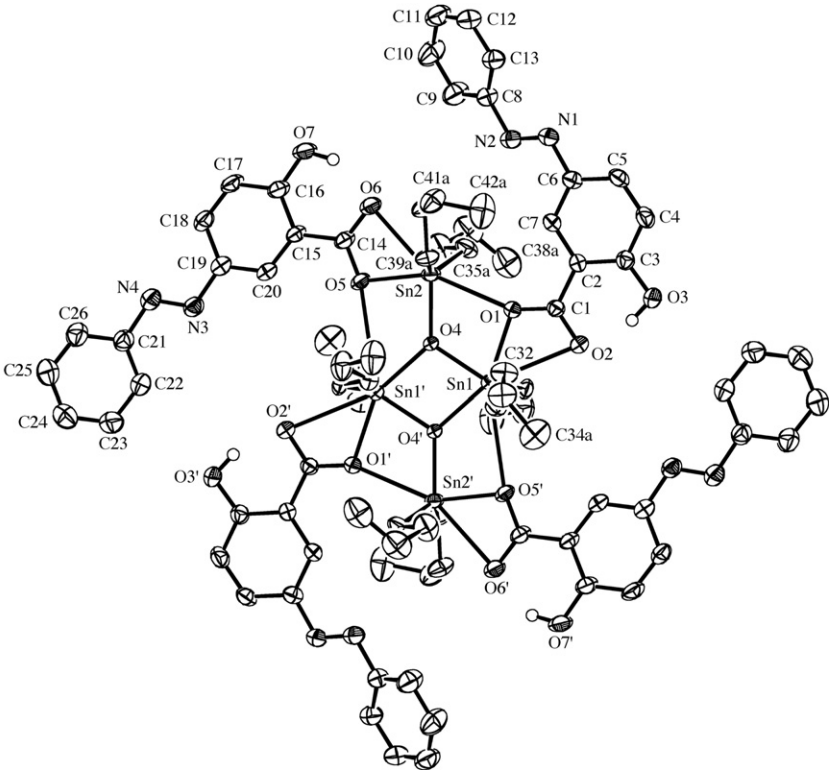

Fig. 2. The molecular structure of $\{[^{n}Bu_2Sn(L^1H)]_2O\}_2$ (**1**) with 50% probability ellipsoids, most H-atoms omitted for clarity and showing only one of the disordered butyl group conformations. The symmetry operator for primed atoms is $1-x, -y, 2-z$.

Sn(1) and Sn(2), respectively. Similarity restraints were applied to the chemically equivalent bond lengths and angles involving all disordered C-atoms.

The hydroxy H-atoms of **1** and **5** were placed in the positions indicated by a difference electron density map and their positions were allowed to refine together with individual isotropic displacement parameters. All other H atoms in the structures were placed in geometrically calculated positions and refined using a riding model where each H atom was assigned a fixed isotropic displacement parameter with a value equal to $1.2U_{eq}$ of its parent C atom ($1.5U_{eq}$ for the methyl groups and for the hydroxy groups of **4** and **6**). The refinement of each structure was carried out on F^2 using full-matrix least-squares procedures, which minimized the function $\sum w(F_o^2 - F_c^2)^2$. Corrections for secondary extinction were not applied. For **1**, four reflections, whose intensities were considered to be extreme outliers, were omitted from the final refinement. All calculations were performed using the SHELXL97 program [28].

2.6. Biological tests

The in vitro cytotoxicity tests on compounds **1** and **4** were performed using the SRB test for the estimation of cell viability. The cell lines WIDR (colon cancer), M19 MEL (melanoma), A498 (renal cancer), IGROV (ovarian cancer) and H226 (non-small cell lung cancer) belong to the currently used anticancer screening panel of the National Cancer Institute, USA [29]. The MCF7 (breast cancer) cell line is estrogen receptor (ER)+/progesterone receptor (PgR)+ and the cell line EVSA-T (breast cancer) is (ER)-/(Pgr)-. Prior to the experiments, a mycoplasma test was carried out on all cell lines and found to be negative. All cell lines were maintained in a continuous logarithmic culture in RPMI 1640 medium with Hepes and phenol red. The medium was supplemented with 10% FCS, 100 μg/ml penicillin and 100 μg/ml streptomycin. The cells were mildly trypsinized for passage and for use in the experiments. RPMI and FCS were obtained from Life technologies (Paisley, Scotland). SRB, DMSO, Penicillin and streptomycin were obtained from Sigma (St. Louis MO, USA), TCA and acetic acid from Baker BV (Deventer, NL), and PBS from NPBI BV (Emmer-Compascuum, NL).

The test compounds **1** and **4** and reference compounds were dissolved to a concentration of 250,000 ng/ml in full medium by 20-fold dilution of a stock solution which contained 1 mg of compounds **1** and **4**/200 μl. Compounds **1** and **4** were dissolved in DMSO. Cytotoxicity was estimated by the microculture sulforhodamine B (SRB) test [30].

2.6.1. Experimental protocol and cytotoxicity tests

The experiment was started on day 0. On day 0, 150 μl of trypsinized tumour cells (1500–2000 cells/well) were plated in 96-wells flat-bottomed microtiter plates (falcon 3072, BD). The plates were preincubated for 48 h at 37 °C, 8.5% CO_2 to allow the cells to adhere. On day 2, a threefold

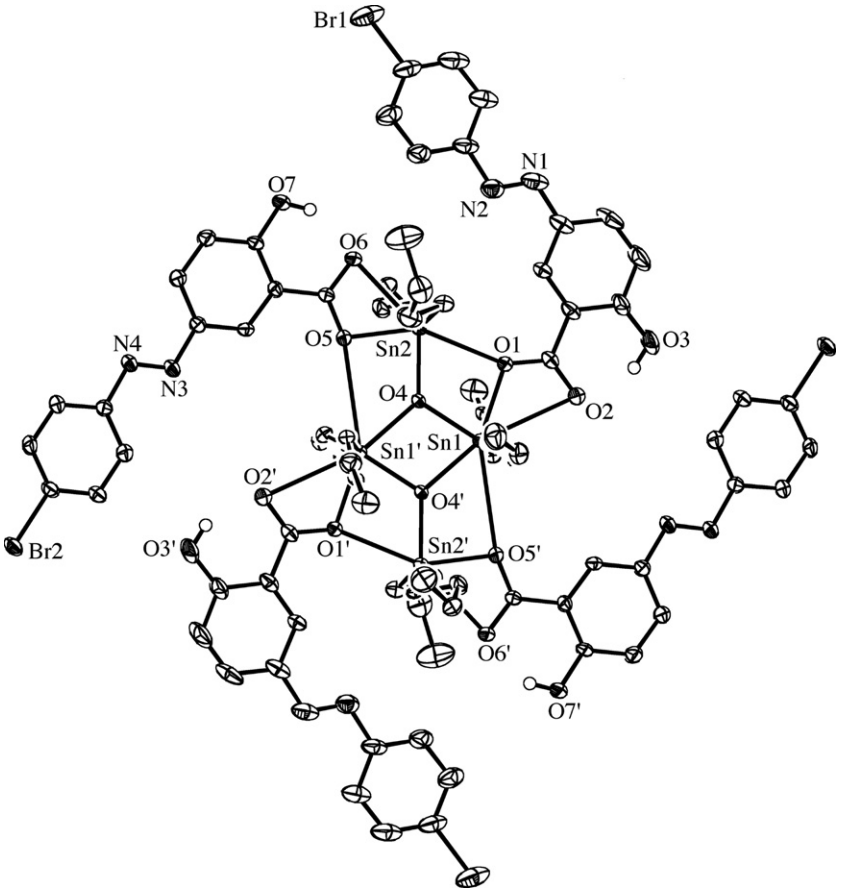

Fig. 3. The molecular structure of $\{[^{n}Bu_2Sn(L^6H)]_2O\}_2$ (**6**) with 50% probability ellipsoids, most H-atoms omitted for clarity and showing only one of the disordered butyl group conformations. The symmetry operator for primed atoms is $-2-x, 2-y, 2-z$.

dilution sequence of ten steps was made in full medium, starting with the 250,000 ng/ml stock solution. Every dilution was used in quadruplicate by adding 50 μl to a column of four wells. This results in a highest concentration of 62,500 ng/ml being present in column 12. Column 2 was used for the blank. To column 1, PBS was added to diminish interfering evaporation. On day 7, washing the plate twice with PBS terminated the incubation. Subsequently, the cells were fixed with 10% trichloroacetic acid in PBS and placed at 4 °C for an hour. After five washings with tap water, the cells were stained for at least 15 min with 0.4% SRB dissolved in 1% acetic acid. After staining, the cells were washed with 1% acetic acid to remove the unbound stain. The plates were air-dried and the bound stain was dissolved in 150 μl (10 mM) tris-base. The absorbance was read at 540 nm using an automated microplate reader (Labsystems Multiskan MS). The data were used for construction of concentration–response curves and the determination of ID_{50} values by use of the Deltasoft 3 software. The in vitro cytotoxicity experiments were carried out at the Laboratory of Experimental Chemotherapy and Pharmacology, Department of Medical Oncology, Erasmus Medical Center, Rotterdam, The Netherlands under the supervision of Dr. K. Nooter and Prof. Dr. G. Stoter.

3. Results and discussion

3.1. Synthesis

The 5-[(*E*)-2-(aryl)-1-diazenyl]-2-hydroxybenzoic acids (LHH′) react with di-*n*-butyltin(IV) oxide in anhydrous toluene in a 1:1 ratio to give compounds of the formulation $\{[^{n}Bu_2Sn(LH)]_2O\}_2$ (**1**–**6**). The complexes were isolated as orange crystalline solids in good yield and purity. They are stable in air and are soluble in common organic solvents.

3.2. Spectroscopy

Diagnostically important infrared absorption frequencies for the carboxylate antisymmetric [ν_{asym}(OCO)] stretching vibration of the complexes appears at 1625 cm^{-1}. The assignment of the symmetric [ν_{sym}(OCO)] stretching vibration band could not be made owing to the complex pattern of the spectra. In addition, a strong broad band at around 625 cm^{-1} was detected for the complexes, which was assigned to the ν(Sn–O–Sn) mode [31,32].

The solution ^1H and ^{13}C NMR data of the ligands have been reported previously [14,15,18,19]. The conclusions

drawn from the ligand assignment have subsequently been extrapolated to complexes **1**–**6** owing to the similarity in the data. The ^{1}H NMR integration values are completely consistent with the formulation of the products. The butyl protons of the compounds are not properly defined and show multiplets and a broad singlet. Further, the low intensities of the Sn–^{n}Bu resonances and a poor signal-to-noise ratio prevented identification of ^{n}J(Sn–C). The methyl protons of the ligand in compound **4** show two signals in the ^{1}H NMR spectrum. This indicates that two types of tin centres are present with non-equivalent surroundings. This was further confirmed by the crystal structure of compound **4** and the ^{119}Sn NMR spectra. In the ^{13}C NMR spectra for the compounds **1** and **4**–**6**, more than one signal is observed for each methylenic carbon atom, while only one signal is observed for the methyl carbon atoms of the butyl group. The ^{119}Sn NMR spectra of the compounds (**1** and **4**–**6**), display a pair of resonances of equal intensities at around −186 and −188 ppm, which confirms the presence of *endo* and *exo* cyclic tin atoms [33,34]. Although it is difficult to assign coordination with certainty to the tin atoms on the basis of their ^{119}Sn chemical shifts, values of δ (^{119}Sn) in the ranges −200 to −400, −90 to −190 and 200 to −60 ppm have been associated with six-, five- and four-coordinate tin centres bearing *n*-butyl groups, respectively [35]. On this basis, two chemically different five-coordinate tin centres (endocyclic and exocyclic) are present in solution for the di-*n*-butyltin complexes, which is consistent with the X-ray crystal structures (vide infra). This shows that the coordination environments of the tin atoms in the solid state are retained in solution. Thus, the ^{13}C and ^{119}Sn NMR data for the complexes (**1** and **4**–**6**), provide reasonable support for the formation of a dimeric tetraorganodistannoxane structure [33,36]. Although two structurally different carboxylate groups are present in the complexes, as revealed by the crystal structure analyses (see below), only single broad resonances are observed for the COO groups in the ^{13}C NMR spectra, which might also correspond to the situation when two ^{13}C resonances from two distinct carboxyl groups exist, but the difference between them is rather small. This could arise in the case of fast intramolecular rearrangement on the NMR time scale, as described by Martins et. al [13]. The ^{119}Sn chemical shifts are much more sensitive to subtle structural changes and the observed difference between the two tin resonances was only about 3 ppm. The difference in ^{13}C resonances should, therefore, be even smaller [34]. This may be due to the accidental magnetic equivalence of the carbonyl carbon atoms on the NMR time scale. On the other hand, compounds **2** and **3** deserve specific mention. In the ^{1}H NMR spectra of these compounds, there were only two sharp signals from residual non-deuterated chloroform and TMS. The other signals both for acidic, aromatic and aliphatic protons were considerably broadened. The acidic proton part of the ^{1}H NMR spectrum of compound **3** measured at three different temperatures is shown in Fig. 4.

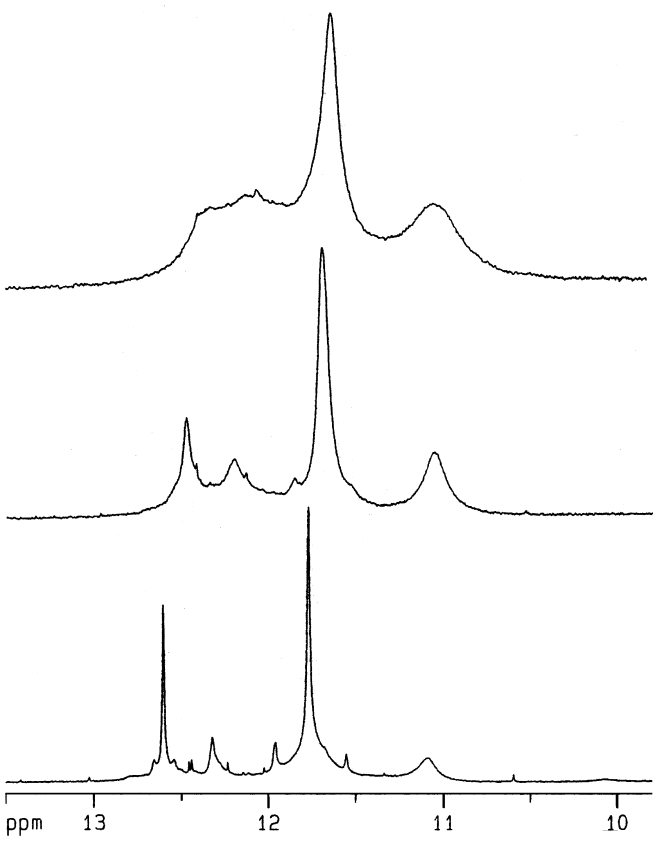

Fig. 4. Acidic protons part of the ^{1}H NMR spectrum of **3** measured at 275 K (bottom trace), 300 K (middle trace) and 325 K (upper trace).

The pattern in the spectrum was completely reconstructed after increasing temperature to 325 K and subsequently decreasing the temperature to 275 K. The aromatic and aliphatic proton signals behaved similarly. It is, thus, clear that both samples undergo very complex exchange processes in deuteriochloroform solution. Each particular resonance in the ^{13}C NMR spectra of compounds **2** and **3** consisted of several lines differing in tenths or hundredths of ppm or the signal was rather broadened. In the ^{119}Sn NMR spectra, there were several resonances of different relative intensities and different line half-widths in the range of −114 to −195 ppm. The reason might be that compounds **2** and **3** are substituted in positions 2′ and 3′ of the phenyl ring (see Fig. 1 for the ligand substitution) while other compounds have substituents in position 4′, which might be less of a hindrance to phenyl group rotation.

The ^{119}Sn Mössbauer spectra of complexes **1**–**6** all show one well resolved single doublet with $\Gamma\pm$ values of 0.79–0.95 mm s^{-1}, which indicates that the four tin centres present in the molecule have a similar environment. The quadrupole splitting (Δ) values lie in the range 3.23–3.49 mm s^{-1}, which is consistent with a five-coordinate or a six-coordinate tin atom [37]. The isomer shifts of the complexes were found in the restricted range 1.31–

1.35 mm s^{-1}, which is typical of quadravalent tin centres [37]. Further, the ratio of the quadrupole splitting value to isomer shift value ($\rho = \Delta/\delta$) indicates coordination greater than four [38]. A similar Δ range was observed recently for the di-*n*-butyltin complexes of analogous mixed ligands having a R_2SnO_4 arrangement, which were also characterized by X-ray crystallography [21]. Thus, the Mössbauer results are consistent with hexa-coordinated tin atoms with a distorted *trans*-R_2Sn octahedral geometry. Furthermore, the Mössbauer results for the present investigation neither distinguish the exo and endocyclic tin centres nor their calculated C–Sn–C angles (the median value was about 135°) obtained from the Parish approach [39].

Unlike common organic and bioorganic molecules (typically $[M+H]^+$ and $[M-H]^-$ ions are produced in the positive-ion and the negative-ion ESI modes, respectively), the ESI mass spectra of organotin compounds containing multiple tin atoms are rather complex and difficult to interpret. The isotopic distributions of polytin ions are very broad, which results in decreased relative abundances of these high-mass ions. To improve the signal-to-noise ratio, the tuning parameter "compound stability" was reduced to 20% in the negative-ion mode and longer averaging of mass spectra was used in both polarity modes. Based on previous experiences with the measurement and spectra interpretation of organotin(IV) compounds [20,34,40], the complex approach was used for the structure confirmation of compounds **1**–**6**. This also involved the following complementary steps: (a) measurements both in positive-ion and negative-ion ESI modes, (b) measurements of all important precursor ions in a series of multistage tandem mass spectrometric experiments, and (c) comparison of theoretical and experimental isotopic distributions for important ions in the spectra. The molecular weight (MW) determination is rather difficult for organotin compounds containing multiple tin atoms because of the extensive number of unusual molecular adducts. However, the measurement in both polarity modes can often provide complementary information for unambiguous MW determination. When the MW is determined, tandem mass spectra (MS/MS and MS^n) experiments are then performed to obtain additional structural information based on characteristic neutral losses observed in MS/MS spectra, such as butene, butane, water, CO_2, ligands, etc. The full list of observed ions together with their *m*/*z* values and interpretation is listed in Section 2.4. A comparison of experimental and theoretical isotopic relative abundances was used for the confirmation of the proposed interpretation of particular ions. The mass spectra of compounds **2**, **3** and **4** are completely identical.

3.3. X-ray crystallography

The crystal structures of compounds **1** and **4**–**6** reveal that the Sn-coordination complex in each case has the basic type **II** structural motif described in the Introduction. Compound **4** crystallizes as a *n*-hexane solvate, while compounds **5** and **6** crystallize as benzene solvates. The coordination complexes are centrosymmetric tetranuclear bis(dicarboxylatotetrabutyldistannoxane) complexes containing a planar Sn_4O_2 core in which two μ_3-oxo O-atoms connect an Sn_2O_2 ring to two exocyclic Sn-atoms to give a $R_8Sn_4O_2$ central unit. Views of the molecular structures of the representative complexes **1** and **6** are shown in Figs. 2 and 3 (see Scheme 1 for line diagrams), while selected geometric parameters are collected in Table 2. The following specific details are given for the structure of **1**, but the comments apply equally well to the other three structures and it is apparent that varying the 4-substituent of the terminal phenyl group of the carboxylate ligands has an insignificant influence on the overall structure of the molecule and the coordination geometry of the Sn-atoms. The exocyclic Sn-atoms [Sn(2)] in **1** have six-coordination, while the endocyclic Sn-atoms [Sn(1)] have seven-coordination, excluding the central Sn···Sn contact of 3.3692(2) Å, although two of the Sn(1)···O distances are very long at 2.910(2) and 3.247(2) Å. The two independent exo-Sn···endo-Sn distances are 3.5562(2) and 3.8102(2) Å. Each exocyclic Sn-atom is bidentate coordinated in an asymmetric fashion by a carboxylate ligand via the two carboxylate O-atoms, with the longer Sn–O interaction being 2.682(2) Å. Additionally, the carboxylate O-atom in each of these ligands involved in the shorter Sn(1)–O bond coordinates via a second very long Sn···O contact [3.247(2) Å] to an endocyclic Sn-atom. The other two carboxylate ligands in the molecule each have asymmetric bidentate coordination via the two carboxylate O-atoms to an endocyclic Sn-atom, with the longer Sn···O interaction being quite long at 2.910(2) Å, and the other carboxylate O-atom in each of these ligands coordinates via a second long Sn–O bond [2.647(2) Å] to an exocyclic Sn-atom. Thus, all carboxylate ligands have very similar modes of coordination, although the pattern of Sn–O distances is not quite the same for each of the two symmetry-independent carboxylate species. In essence, one carboxylate O-atom in each ligand bridges asymmetrically both structurally unique Sn-atoms, while the other carboxylate O-atom coordinates with a longer Sn–O distance to just one of the Sn-atoms. This latter O-atom is always that which is closest to the hydroxy group of the ligand and which thereby acts as an acceptor for an intramolecular hydrogen bond from the hydroxy group.

Each Sn-atom is also coordinated by two butyl groups, which in some of the structures display disorder (see Section 2.5). The positions of the butyl ligands are reminiscent of a *trans*-R_2Sn geometry, although the C–Sn–C angles (Table 2) deviate significantly from 180°. The Sn_4O_2 core and carboxylate ligands form an essentially planar system with the butyl groups extending roughly perpendicular to this plane. The highly irregular coordination environment about each Sn-atom, in part caused by the restrictions of the bite angles of the carboxylate ligands and their bridging function, makes it awkward to use terms like pentagonal bipyramidal or octahedral to describe the geometry of the coordination spheres of atoms Sn(1) and Sn(2), respectively. If the longer

Table 2
Selected interatomic distances (Å) and angles (°) for compounds **1** and **4**–**6**[a]

	1	4	5	6
Sn(1)–O(1)	2.234(2)	2.265(3)	2.247(2)	2.249(4)
Sn(1)–O(2)	2.910(2)	3.107(3)	3.006(2)	2.991(6)
Sn(1)–O(4)	2.044(2)	2.054(2)	2.051(2)	2.047(4)
Sn(1)–O(4)^{i}	2.171(2)	2.165(2)	2.171(2)	2.174(3)
Sn(1)–O(5)^{i}	3.247(2)	3.158(3)	3.217(2)	3.218(4)
Mean Sn(1)–C	2.131(8)	2.122(5)	2.124(4)	2.12(3)
Sn(2)–O(1)	2.647(2)	2.616(3)	2.621(2)	2.616(5)
Sn(2)–O(4)	2.011(2)	1.998(2)	2.005(2)	2.016(4)
Sn(2)–O(5)	2.124(2)	2.103(3)	2.124(2)	2.125(4)
Sn(2)–O(6)	2.682(2)	2.658(3)	2.672(2)	2.681(4)
Mean Sn(2)–C	2.125(6)	2.122(5)	2.124(4)	2.16(3)
Sn(1)···Sn(1)^{i}	3.3692(2)	3.3716(7)	3.3729(3)	3.3758(8)
O(1)–Sn(1)–O(4)	76.40(6)	74.82(9)	75.47(7)	75.2(1)
O(1)–Sn(1)–O(4)^{i}	150.28(6)	148.74(9)	149.37(7)	149.0(1)
O(4)–Sn(1)–O(4)^{i}	73.91(7)	74.0(1)	73.98(8)	73.9(2)
Mean C–Sn(1)–C	133.3(8)	133.0(2)	132.0(1)	131.5(8)
O(1)–Sn(2)–O(4)	67.76(6)	67.95(9)	67.96(7)	67.7(2)
O(1)–Sn(2)–O(5)	151.48(6)	150.44(9)	151.18(7)	150.8(1)
O(1)–Sn(2)–O(6)	155.40(6)	155.99(8)	155.76(6)	155.8(1)
O(4)–Sn(2)–O(5)	83.73(7)	82.50(9)	83.28(7)	83.2(1)
O(4)–Sn(2)–O(6)	136.78(6)	135.94(9)	136.28(7)	136.5(2)
O(5)–Sn(2)–O(6)	53.10(6)	53.54(9)	53.04(7)	53.4(1)
Mean C–Sn(2)–C	132(1)	131.6(2)	131.4(1)	131(3)
Sn(1)–O(1)–Sn(2)	93.15(6)	93.72(9)	93.72(7)	94.1(2)
Sn(1)–O(4)–Sn(1)^{i}	106.09(7)	106.1(1)	106.02(8)	106.2(2)
Sn(1)–O(4)–Sn(2)	122.56(8)	123.5(1)	122.84(9)	123.0(3)
Sn(2)–O(4)–Sn(1)^{i}	131.29(8)	130.4(1)	131.06(9)	130.8(2)

[a] Symmetry operation i moves the specified atom through the molecular crystallographic centre of inversion.

Sn···O distances (>2.7 Å) are ignored in considering the primary coordination sphere, the appearance of a regular coordination polyhedron remains elusive. Nonetheless, the environment about atom Sn(1) can be envisaged as a quite distorted trigonal bipyramid in which O(4) and the butyl ligands occupy the equatorial plane and the axial O-atoms are bent well away from linearity at around 150° (Table 2). The environment about atom Sn(2) can be described as a distorted skew-trapezoidal bipyramid with the butyl ligands occupying axial positions, but where the C–Sn(2)–C axis is bent to about 132° so as to position these ligands more above the open side of the trapezoidal plane occupied by the longer Sn(2)–O(1) and Sn(2)–O(6) carboxylate distances. In all four of the structures reported here, the Sn(2)–O(1) and Sn(2)–O(6) distances are almost equal. In a closely related structure with *p*-fluorophenylacetate ligands [6], the corresponding distances are less symmetrical at 2.498(5) and 2.746(6) Å, respectively, and it was debated as to whether or not the latter contact should be considered as part of the coordination sphere of atom Sn(2). The occurrence of a more symmetrical arrangement in **1** and **4**–**6** adds weight to the argument for including both interactions in the assessment of the coordination geometry.

The type **II** structural motif displayed by compounds **1** and **4**–**6** occurs less frequently than the more common type **I** motif. The Cambridge Structural Database [41] records 104 structures that have the $R_8Sn_4O_2$ core, but only 11 of these have the type **II** motif. All of these type **II** molecules have very a similar geometry within the central $R_8Sn_4O_2$ core and there is little variation among the various Sn–O distances. Usually, the Sn(2)–O(1) and Sn(2)–O(6) distances are slightly asymmetric and of approximately the same magnitude as in the *p*-fluorophenylacetate derivative [6]. The more symmetrical nature of these distances in **1** and **4**–**6** seems to be unique amongst the structures that have purely organic carboxylate ligands. There is a ferrocenoylpropionate derivative in which both distances are close to 2.72 Å, but the adjacent ferrocene group in each ligand may have an impact on the Sn–O distances [42].

3.4. In vitro cytotoxicity

Recently, we have reported in vitro cytotoxic results on the diorganotin dicarboxylate compound $^{n}Bu_2Sn(L^2H)_2$ (L^2H = deprotonated ligand, refer to Fig. 1) where the Sn coordination geometry was skew-trapezoidal bipyramidal [20]. The results of the in vitro cytotoxicity test in human tumour cell lines on compounds **1** and **4** are given as ID_{50} values in Table 3 and compared with the data for $^{n}Bu_2Sn(L^2H)_2$ and some compounds that are in current clinical use as antitumour agents. The table clearly shows that compounds **1** and **4** are more active in vitro than $^{n}Bu_2Sn(L^2H)_2$ and most of the standard drugs against all seven human cancer cell lines. This encouraging cytotoxic effect may be predictive of in vivo antitumour activity. Compounds **1** and **4** may be suitable candidates for modification in order to improve cytotoxic and dissolution properties. Although compounds **1** and **4** possess quite high

Table 3
ID_{50} values (ng/ml) of test compounds in vitro using SRB as cell viability test

Test compound[a]	Cell lines						
	A498	EVSA-T	H226	IGROV	M19 MEL	MCF-7	WIDR
1	135	14	205	149	52	27	116
4	140	14	217	155	54	29	115
$^{n}Bu_2Sn(L^2H)_2$	387	63	337	179	122	124	359
$\{[^{n}Bu_2(RCOO)Sn]_2O\}_2$[b]	<3	<3	5	<3	<3	<3	6
DOX	90	8	199	60	16	10	11
CPT	2253	422	3269	169	558	699	967
5-FU	143	475	340	297	442	750	225
MTX	37	5	2287	7	23	18	<3.2
ETO	1314	317	3934	580	505	2594	150
TAX	<3.2	<3.2	<3.2	<3.2	<3.2	<3.2	<3.2

[a] Abbreviation for the reference drugs: DOX = doxorubicin, CPT = cisplatin, 5-FU = 5-fluorouracil, MTX = methotrexate, ETO = etoposide and TAX = paclitaxel.
[b] R = $CH_3OCH_2CH_2OCH_2$ [43].

in vitro cytotoxicity, it should be noted that di-*n*-butyltin 3,6-dioxaheptanoates and 3,6,9-trioxadecanoates, having the same formulations, are even more cytotoxic [43]. For comparison, an example is added in Table 3. It is well known that clinically active platinum compounds show different in vitro cytotoxicity due to slight differences in kinetic and mechanistic behaviour. It has also been suggested that organotin compounds interact with DNA at the level of the phosphate group, which may be followed by intercalation of a ligand into DNA [44,45]. Different active organotin compound may still show slight variation in in vitro cytotoxicity due to different kinetic and mechanistic behaviour.

Acknowledgements

The financial support of the Department of Science and Technology, New Delhi, India (Grant No. SP/S1/IC-03/2005, TSBB), the Czech Science Foundation (Grant No. 203/03/1118, AL) and the Ministry of Education, Youth and Sports of the Czech Republic (Project No. MSM0021627502, MH) are gratefully acknowledged. R.J.B. acknowledges the DoD-ONR for funds to upgrade the diffractometer and also the ONR/ASEE program for Summer Faculty Fellowships at the Naval Research Laboratory. E.R. is indebted to the Università di Palermo, Italy for support.

Appendix A. Supplementary material

Views of the molecular structures of $\{[^{n}Bu_2Sn(L^4H)]_2O\}_2$ (**4**) and $\{[^{n}Bu_2Sn(L^5H)]_2O\}_2$ (**5**). CCDC-601854–CCDC-601857 contain the supplementary crystallographic data for complexes **1** and **4**–**6**, respectively. These data can be obtained free of charge from The Cambridge Crystallographic Data Centre via www.ccdc.cam.ac.uk/data_request/cif. Supplementary data associated with this article can be found, in the online version, at doi:10.1016/j.jorganchem.2006.08.005.

References

[1] J. Makarevic, M. Jokic, B. Peric, V. Tomisic, B. Kojic-Prodic, M. Zinic, Chem. Eur. J. 7 (2001) 3328.
[2] H. Zhang, X. Wang, H. Zhu, W. Xiao, K. hang, B.K. Teo, Inorg. Chem. 38 (1999) 886.
[3] J. Hagrman, D. Hagrman, J. Zubieta, Angew. Chem. Int. Ed. 38 (1999) 2638.
[4] (a) M. Gielen, Appl. Organomet. Chem. 16 (2002) 481;
(b) M. Gielen, M. Biesemans, R. Willem, Appl. Organomet. Chem. 19 (2005) 440.
[5] M. Eddaoudi, D.B. Moler, H. Li, B. Chen, T.M. Reineke, M. O'Keeffe, O.M. Yaghi, Acc. Chem. Res. 34 (2001) 319, and references therein.
[6] E.R.T. Tiekink, M. Gielen, A. Bouhdid, M. Biesemans, R. Willem, J. Organomet. Chem. 494 (1995) 247.
[7] F. Ribot, C. Sanchez, A. Meddour, M. Gielen, E.R.T. Tiekink, M. Biesemans, R. Willem, J. Organomet. Chem. 552 (1998) 177.
[8] V.S. Petrosyan, N.S. Yashina, T.V. Drovetskaia, A.V. Yatsenko, L.A. Aslanov, L. Pellerito, Appl. Organomet. Chem. 10 (1996) 523.
[9] J.A. Blie, R.A. Howie, J.L. Wardell, P.J. Cox, Polyhedron 16 (1997) 881.
[10] E.R.T. Tiekink, Appl. Organomet. Chem. 5 (1991) 1;
E.R.T. Tiekink, Trends Organomet. Chem. 1 (1994) 71.
[11] M. Yakoo, J. Ogura, T. Kanzawa, J. Polym. Sci., Polym. Lett. Ed. 5 (1967) 57.
[12] T. Yano, K. Nakashima, J. Otera, R. Okawara, Organometallics 4 (1985) 1501.
[13] J.C. Martins, M. Biesemans, R. Willem, Progr. NMR Spectrosc. 36 (2000) 271.
[14] T.S. Basu Baul, S. Dhar, N. Kharbani, S.M. Pyke, R. Butcher, F.E. Smith, Main Group Met. Chem. 22 (1999) 413.
[15] T.S. Basu Baul, S. Dhar, S.M. Pyke, E.R.T. Tiekink, E. Rivarola, R. Butcher, F.E. Smith, J. Organomet. Chem. 633 (2001) 7.
[16] T.S. Basu Baul, W. Rynjah, E. Rivarola, A. Linden, J. Organomet. Chem. 690 (2005) 613.
[17] T.S. Basu Baul, W. Rynjah, K.S. Singh, C. Pellerito, P. D'Agati, L. Pellerito, Appl. Organomet. Chem. 19 (2005) 1189.
[18] T.S. Basu Baul, S. Dhar, E.R.T. Tiekink, Main Group Met. Chem. 24 (2001) 293.
[19] T.S. Basu Baul, S. Dhar, E. Rivarola, F.E. Smith, R. Butcher, X. Song, M. McCain, G. Eng, Appl. Organomet. Chem. 17 (2003) 261.
[20] T.S. Basu Baul, W. Rynjah, R. Willem, M. Biesemans, I. Verbruggen, M. Holčapek, D. de Vos, A. Linden, J. Organomet. Chem. 689 (2004) 4691.
[21] T.S. Basu Baul, W. Rynjah, E. Rivarola, C. Pettinary, A. Linden, J. Organomet. Chem. 690 (2005) 1413.

[22] R. Hooft, KappaCCD Collect Software, Nonius BV, Delft, The Netherlands, 1999.
[23] Z. Otwinowski, W. Minor, in: C.W. Carter Jr., R.M. Sweet (Eds.), Methods in Enzymology, Macromolecular Crystallography, Part A, vol. 276, Academic Press, New York, 1997, pp. 307–326.
[24] R.H. Blessing, Acta Crystallogr. Sect. A 51 (1995) 33.
[25] A. Altomare, G. Cascarano, C. Giacovazzo, A. Guagliardi, M.C. Burla, G. Polidori, M. Camalli, SIR92, J. Appl. Crystallogr. 27 (1994) 435.
[26] Bruker programs SMART, SAINT, SHELXTL and SADABS. Bruker AXS Inc., Madison, WI, USA, 2001.
[27] G.M. Sheldrick, SHELXS97, Program for the Solution of Crystal Structures, University of Göttingen, Germany, 1997.
[28] G.M. Sheldrick, SHELXL97 Program for the Refinement of Crystal Structures, University of Göttingen, Germany, 1997.
[29] M.R. Boyd, Principles Pract. Oncol. 3 (1989) 1.
[30] Y.P. Keepers, P.E. Pizao, G.J. Peters, J. Van Ark-Otte, B. Winograd, H.M. Pinedo, Eur. J. Cancer 27 (1991) 897.
[31] T.P. Lockhart, F. Davidson, Organometallics 6 (1987) 2471.
[32] J.A. Zubieta, J.J. Zuckerman, Prog. Inorg. Chem. 24 (1987) 251.
[33] T. Yano, K. Nakashima, J. Otera, R. Okawara, Organometallics 4 (1985) 1501.
[34] T.S. Basu Baul, C. Masharing, S. Basu, E. Rivarola, M. Holčapek, R. Jirásko, A. Lyčka, D. de Vos, A. Linden, J. Organomet. Chem. 691 (2006) 952.
[35] J. Holeček, M. Nádvorník, K. Handlíř, A. Lyčka, J. Organomet. Chem. 315 (1986) 299.
[36] A.G. Davies, L. Smith, P.J. Smith, W. McFarlane, J. Organomet. Chem. 24 (1971) 245.
[37] R. Barbieri, F. Huber, L. Pellerito, G. Ruisi, A. Silvestri, in: P.J. Smith (Ed.), ^{119}Sn Mössbauer Studies on Tin Compounds: Chemistry of Tin, 2nd ed., Blackie Academic & Professional, London, 1998, pp. 496–540.
[38] R.H. Herber, H.A. Stockler, W.T. Reichle, J. Chem. Phys. 42 (1965) 2447.
[39] R.V. Parish, Structure and bonding in tin compounds, in: G.J. Long (Ed.), Mössbauer Spectroscopy Applied to Inorganic Chemistry, Plenum Press, New York, 1984, pp. 527–575, Chapter 16.
[40] L. Kolářová, M. Holčapek, R. Jambor, L. Dostál, A. Růžička, M. Nádvorník, J. Mass Spectrom. 39 (2004) 621.
[41] F.H. Allen, Acta Crystallogr. Sect. B 58 (2002) 380.
[42] B. Peng, L.-J. Sun, W.-X. Chang, Q.-L. Xie, Chinese J. Struct. Chem. 22 (2003) 647.
[43] M. Kemmer, M. Gielen, M. Biesemans, D. de Vos, R. Willem, Metal-Based Drugs 5 (1998) 189.
[44] Q. Li, P. Yang, H. Wang, M. Guo, J. Inorg. Biochem. 64 (1996) 181.
[45] A. Casini, L. Messori, P. Orioli, M. Gielen, M. Kemmer, R. Willem, J. Inorg. Biochem. 85 (2001) 297.